THE APPLICATION OF GEOSTATISTICAL SEISMIC INVERSION FOR DELINEATING THIN RESERVOIRS: A CASE STUDY OF THE JAMBI SUB-BASIN

Abdul Haris[1*], Aditya Dwi Prasetio[2], Agus Riyanto[1], Sri Mardiyati[3]

[1]*Geology Study Program, FMIPA, Universitas Indonesia, Kampus UI Depok, Depok 16424, Indonesia*
[2]*Reservoir Geophysics Graduate Program, Physics Department, FMIPA, Universitas Indonesia, Jl. Salemba Raya No. 4, Jakarta 10430, Indonesia*
[3]*Department of Mathematics, FMIPA, Universitas Indonesia, Kampus UI Depok, Depok 16424, Indonesia*

ABSTRACT

Geostatistical seismic inversion has been successfully carried out to characterize a thin reservoir of the Air Benakat Formation in Indonesia's Jambi sub-basin. The objective of this paper is to characterize detailed P-impedance of the thin reservoir in the Jambi sub-basin using geostatistical seismic inversion rather than deterministic seismic inversion. Geostatistical seismic inversion is believed to be able to enhance vertical resolution and accurately map sub-seismic features. This algorithm uses a geostatistical model, which is constrained by probability density function and a variogram as the input models. The method was applied to eight wells and three-dimensional seismic data that consist of 198 inline and 261 crossline. Prior to performing geostatistical seismic inversion, sensitivity analysis was carried out by cross-plotting petrophysical data to identify the petrophysical properties of the reservoir target. The geostatistical seismic inversion considered 50 realization models that were used as inputs in estimating the probability of the existing subsurface layer and the calculated P-impedance models to obtain the most probable P-impedance model that is useful for characterizing the detailed thin reservoir of the Air Benakat Formation in the Jambi sub-basin. The geostatistical seismic inversion results show a higher resolution of P-impedance compared to the deterministic seismic inversion and are able to resolve thin reservoirs below tuning thickness. In addition, this method is able to optimize better correlation between seismic and petrophysical properties of the thin reservoir with an average thickness below five metres, which is well modelled with reference to both seismic and well data.

Keywords: Air Benakat Formation; Geostatistical seismic inversion; Jambi sub-basin; Thin reservoir

1. INTRODUCTION

The resolving power of seismic data is highly dependent on the seismic bandwidth, which is generally lacking low frequencies and high frequencies. Seismic inversion is one of the most powerful techniques to broaden the seismic bandwidth by adding the low- and high-frequency content. In addition, seismic inversion is able to integrate the seismic and well log data to generate a quantitative geological model of the reservoir, including the P-impedance (Mukerji

et al., 2001; Lang & Grana, 2017). This geological model is directly related to the layer properties rather than the interface properties, which is associated with geological data such as lithology, porosity, and net pay. Therefore, the quantitative geological model has been recognized as an industrial tool for reservoir characterization.

The seismic data contain reflection information that is associated with a P-impedance change in the subsurface (Avseth et al., 2005). The reflection data is transformed into geological information that is laterally and vertically distributed (Bacon et al., 2003; Haris et al., 2017). The development of seismic inversion techniques has been very fast, and there have been varying options for algorithms coming from the conventional up to the superior algorithm (Haris et al., 2018). A conventional algorithm such as sparse-spike of deterministic seismic inversion is only generating a single P-impedance model, which is useful for figuring out general features of the potential reservoir (Shrestha & Boeckmann, 2002; Francis, 2005). Further, sparse-spike of deterministic seismic inversion tends to produce smooth a P-impedance model that minimizes its variability due to the frequency limitation of the real seismic data. The new approach of geostatistical seismic inversion is applied to improve the limitation of deterministic inversion.

Geostatistical seismic inversion is the superior algorithm that considers the stochastic method by using Sequential Gaussian Simulation to solve non-uniqueness problems via statistical analysis to produce equally probable models (Sancevero et al., 2008; Bosch et al., 2010). This algorithm produces a high vertical resolution for imaging thin reservoirs (Torres et al., 1999). Therefore, selecting the geostatistical seismic inversion algorithm is crucial for characterizing the detailed thin reservoir of the Air Benakat Formation in the Jambi sub-basin.

In this work, we applied geostatistical seismic inversion to delineate a thin reservoir of the Air Benakat Formation in the Jambi sub-basin part of the South Sumatra Basin. The study area has a hydrocarbon potential to be explored (Bishop, 2001; Ginger & Fielding, 2005). The purpose of this paper is to increase vertical resolution and to accurately map sub-seismic features of the thin layer reservoir using a geostatistical model where probability density function (PDF) and a variogram as one of the input models. We demonstrate the comparison between the result of the deterministic seismic inversion and the result of the geostatistical seismic inversion.

2. METHODOLOGY

The detailed characterization of the thin reservoir of the Air Benakat Formation in the Jambi sub-basin was carried out by applying geostatistical seismic inversion. To get a better understanding of the advantage of geostatistical seismic inversion, we compared its result to the deterministic seismic inversion result. These two seismic inversion algorithms were applied to three-dimensional post-stack seismic data and data from eight wells. Each well contains gamma ray, density, neutron porosity, sonic, and resistivity data. This work was performed using CGG Jason software. A well–seismic tie was applied to eight wells, and we obtained the average of the correlation coefficient of 0.75. This means that the seismic and well data have a good match in terms of geological data and seismic features.

The deterministic seismic inversion is based on the Constrained Sparse Spike Inversion for calculating P-impedance over the entire survey area (trace gate), which is a type of trace-based inversion. This inversion was based on the convolutional model between the reflection coefficient and seismic wavelet. To reduce the uncertainty, a low-frequency model was used as a guide. This low-frequency model was built from the low-pass filter of P-impedance log interpolation and used the geological horizon as a guide.

Geostatistical inversion inverts the reflection seismic data with the most complex geostatistical algorithm (Havelia et al., 2017). The essential step in this inversion is the geostatistical modelling that generates the PDF and experimental variogram from well data in every target reservoir (Haas & Dubrule, 1994; Sulistiono et al., 2015). The step is continued by simulating the number of initial models based on the PDF and variogram (Robinson, 2001). The initial models were analysed and we decided the best parameter to be chosen. We had to pay much attention to the decisive step of the geostatistical seismic inversion by setting the noise level and sampling rate.

The key differences between the deterministic and geostatistical seismic inversion were in the realization model, as the deterministic seismic inversion only resulted in one P-impedance model, whereas geostatistical inversion resulted in multiple P-impedance models (Sams & Saussus, 2010; Nunes et al., 2017). The multiple models of realization provided the quantity of the non-uniqueness and uncertainty of the inversion result (Francis, 2006; McCrank et al., 2009). The geostatistical inversion was generating a realization model that was bounded by the probability density function from seismic and well data. The uncertainty model was determined based on the multiple realizations model.

3.   RESULTS AND DISCUSSION

In this work, we applied the two seismic inversion algorithms to data from eight wells and three-dimensional seismic data that consisted of 198 inline and 261 crossline. Prior to performing the seismic inversion, a feasibility study was carried out to analyze the P-impedance dimension in the target zone (Hermana et. al., 2017). This feasibility study defined the cutoff value of P-impedance to separate the target zone (sand) and non-target zone (shale). The cutoff value of the gamma rays was defined at 90 American Petroleum Institute (API) units , and the target zone was indicated by a gamma ray measurement of less than 90 API. Moreover, the resistivity cutoff was 2.5 ohms with the target zone indicated by resistivity higher than 2.5 ohms. The cutoff value of P-impedance, which was correlated to gamma rays (y-axis) and resistivity (color) as shown in Figure 1, was defined at 25,000 gr/cc·ft/s. This means the lithology with a P-impedance higher than the cutoff was classified as a reservoir, and the lithology with a P-impedance lower than the cutoff was considered as a non-reservoir.
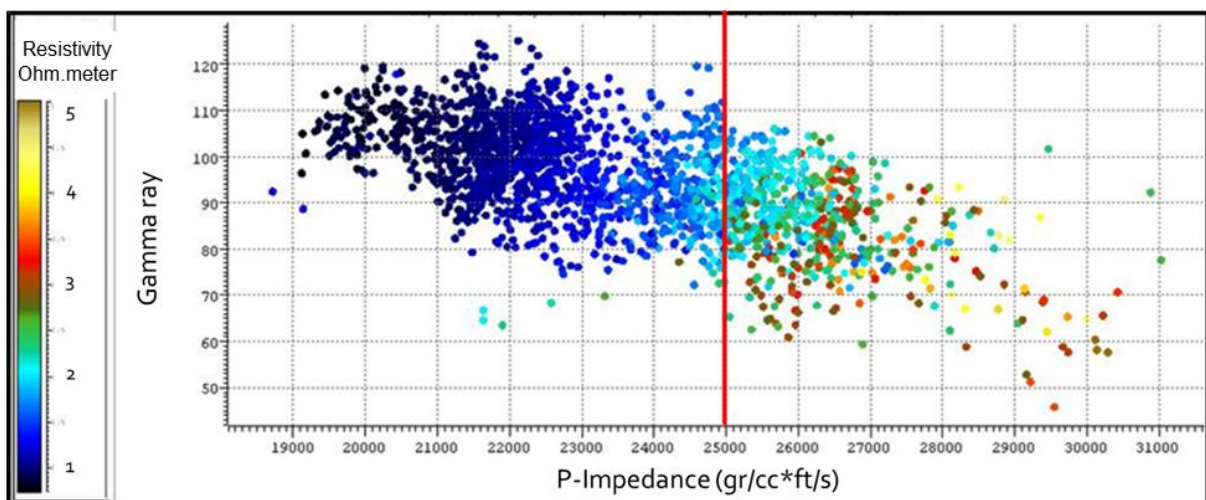
Figure 1 Cross-plot with P-impedance as the x-axis, gamma rays as the y-axis, and resistivity as color. P-impedance cutoff was defined at 25,000 gr/cc·ft/s (red line)

This P-impedance cutoff was correlated to a low gamma ray (less than 90 API) measurement and high resistivity (greater than 2.5 ohms), which represents the sand lithology and the hydrocarbon bearing. The reservoir target was indicated by high impedance because the lithology types of the reservoir were glauconitic sand with higher mineral density and hardened facies. The hardness of the reservoir rock has a direct effect on the acoustic wave propagation.

The geostatistical seismic inversion relied on vertical and lateral variograms. The vertical variogram was determined from data from eight well logs, whereas the lateral variogram was defined by P-impedance (the result of deterministic seismic inversion). Figure 2 shows the vertical and lateral variograms for layer M, which was an exponential-type variogram. This exponential-type variogram was chosen in order to obtain more variation of the thin feature. Figure 2a illustrates the PDF of the relation between P-impedance and porosity from data from eight well logs. The target data is indicated in yellow and the non-target data is marked in green. The data with a high PDF is clustered in a small curve (shown in green). Figure 2b displays the vertical variogram from data from eight well logs; its range was determined at 10 metres. Figure 2c presents the lateral variogram; its range was defined at 1200 metres. This defined variogram was then used as input for the geostatistical seismic inversion.

After completing geostatistical modeling, a simulation of the reservoir model was performed using a Monte Carlo Markov Chain method. This step was for generating initial models by simulating random number well log data in the variogram and PDF. This initial model was built based on an iteration using the Monte Carlo Markov Chain algorithm. Each initial model resulted in one realization of an inversion result and discrete properties model. In this work, we performed the simulation 50 times; thereby, the most probable model was determined based on the average of 50 simulated models. Thus, the probability model was calculated based on these 50 models, then this probability model being quantification of the uncertainty.

(a)　　　　　　　　　　　　　(b)　　　　　　　　　　　　　(c)
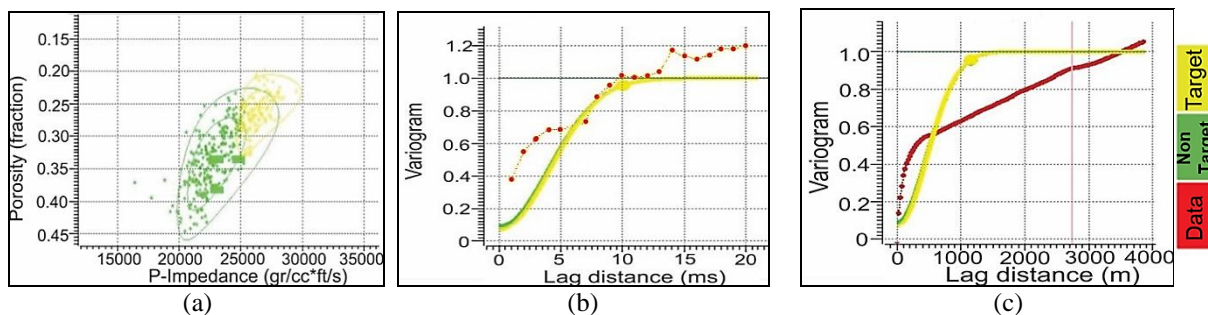
Figure 2 The statistical analysis for layer M that consists of: (a) the probability density function; (b) vertical variogram from porosity data; and (c) lateral variogram from P-impedance data (gr/cc·ft/s). The red, green, and yellow colors indicate the experimental, non-target, and target variogram models, respectively

Figure 3 shows the seismic inversion result from the geostatistical and deterministic seismic inversions. The figure illustrates the different results from these two algorithms. The geostatistical seismic inversion produced higher resolution P-impedance and was able to display the sub-layer features that the deterministic seismic inversion was unable to resolve it. The thin reservoir in layer M was clearly identified in the geostatistical inversion results, which was correlated to the presented sub-layer in the ADP-10 and ADP-19 wells (ellipse (a) in Figure 3) rather than in the deterministic seismic inversion result (ellipse (c) in Figure 3). This thin reservoir was difficult to directly identify by the seismic section, but it could be detected by well log data. In addition, the thicker reservoir (ellipse (b) in Figure 3) in layer N was clearly and continuously imaged in the geostatistical seismic inversion result rather than in the

deterministic seismic inversion result (ellipse (d) in Figure 3).
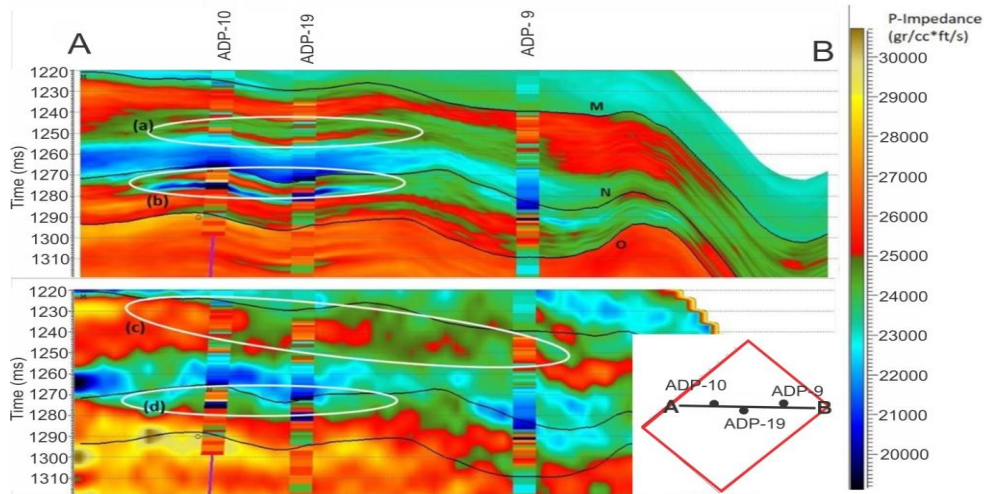
Figure 3 The comparison between the geostatistical seismic inversion result (top) and deterministic seismic inversion result (bottom) for line AB, where the inserted well log data are P-impedance. The ADP-09 well was not included in the inversion process, but it was used to verify the inversion result

The evaluation of the seismic inversion result was not only focused on the resolving power, but also on predicting the inversion result. Thus, we carried out a blind test analysis over data from one well. The ADP-09 well was not included in the inversion process, but it was used to verify the inversion result. Figure 3 shows the advantage of geostatistical seismic inversion in predicting the inversion result compared to the deterministic seismic inversion. The geostatistical seismic inversion result indicated a better match with the ADP-09 well than the deterministic seismic inversion result. This good match was confirmed by the high correlation coefficient and low root means square (RMS) error compared to the deterministic seismic inversion. The geostatistical seismic inversion had a correlation coefficient of 0.512 and an RMS error of 2414.5 gr/cc·ft/s with respect to P-impedance of well log data. In contrast, the deterministic seismic inversion had a correlation coefficient of 0.472 and an RMS error of 2523.4 gr/cc·ft/s.

(a) (b)
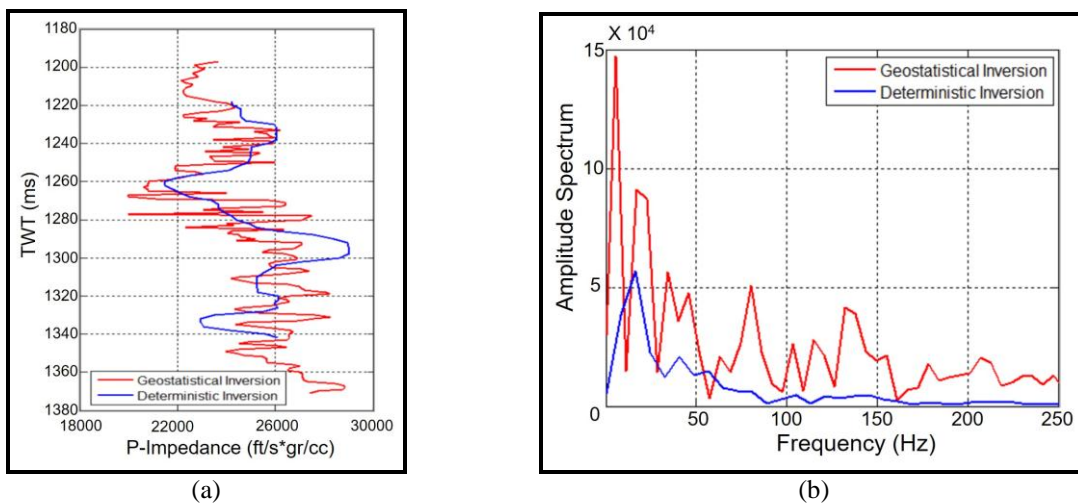
Figure 4 The comparison of: (a) the predicted P-impedance; and (b) the frequency spectra

The advantage of the geostatistical seismic inversion is clearly seen in Figure 4, which

illustrates the comparison of the predicted P-impedance and the frequency spectrum. The target zone's depth range varied from 1200 to 1380 metres, with the red and blue curve showing the geostatistical and deterministic inversion results, respectively. Figure 4a shows the P-impedance of both algorithms that vary from 2000 to 29,000 gr/cc·ft/s. However, it can clearly be seen that geostatistical seismic inversion produces more detailed P-impedance in terms of vertical variation. Furthermore, the spectrum frequency analysis showed that the geostatistical seismic inversion had a higher amplitude spectrum compared to the deterministic seismic inversion, as shown in Figure 4b. These two pieces of evidence verified that the geostatistical seismic inversion produced detail-scale heterogeneities of P-impedance by offering higher resolution rather than the deterministic seismic inversion.

Detailed analysis of the geostatistical seismic inversion result was performed by quantifying the probability model. Figure 5 shows a cross-section of the probability model based on the geostatistical seismic inversion. The thin reservoir in layer M in Figure 3 ellipse (a) has a probability of 60% for the existence of the layer based on the probability model, which is shown in Figure 5. The thicker reservoir in layer N (ellipse (b) in Figure 3) indicates a probability of 80%. These predictive probabilities were based on 50 realizations.

Comparing the P-impedance to the probability model, we can conclude that the variogram has been satisfactorily distributing the well data. The probability model was a combination of the geostatistical model and seismic data; thus, the realization is not continuous because of the non-continuity of the seismic reflection. In general, the geostatistical seismic inversion provided a more geologically reasonable realization than the deterministic seismic inversion.
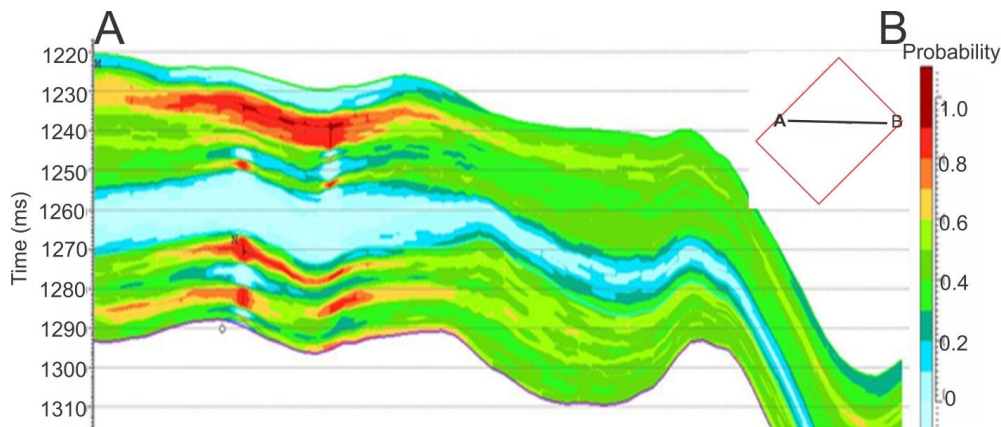
Figure 5 The probability model for line AB, which was produced based on 50 realizations. The black ellipse shows the target reservoir

Further detailed analysis of the geostatistical seismic inversion result was performed by observing the discrete properties model. Figure 6 shows the discrete properties model, which is illustrated in contrasting colors to differentiate the target zone (sand) and non-target zone (clay). The sand reservoir is indicated in yellow and the clay is illustrated in green. The discrete properties model indicated a good match with all available wells, including the ADP-09 well that was used as a blind test. In general, the reservoir, whether thin or thick, was delineated very well in the discrete properties model.

The discrete properties model was determined to be the most probable model based on 50 inverse realizations. Therefore, this model represents the highest probability of determining the sub-surface reservoir distribution. The thin layer under tuning thickness can be identified using this discrete properties model. This means that the thin layer has been successfully distributed via geostatistical seismic inversion. The continuity of the thin reservoir in layer M was

definitely distributed, but it can be improved by incorporating the ADP-09 well into the inversion process. In addition, by increasing the range value in the lateral variogram, the thin reservoir can be extended. However, the uncertainty of the model was increasing as a consequence of increasing the range values.
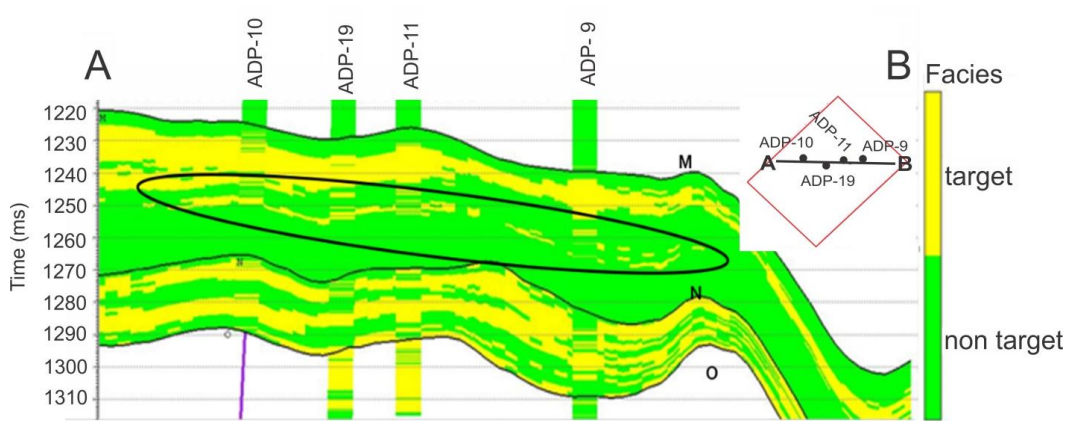
Figure 6 The discrete properties model for line AB. The black ellipse shows the thin reservoir.

(a)

(b)
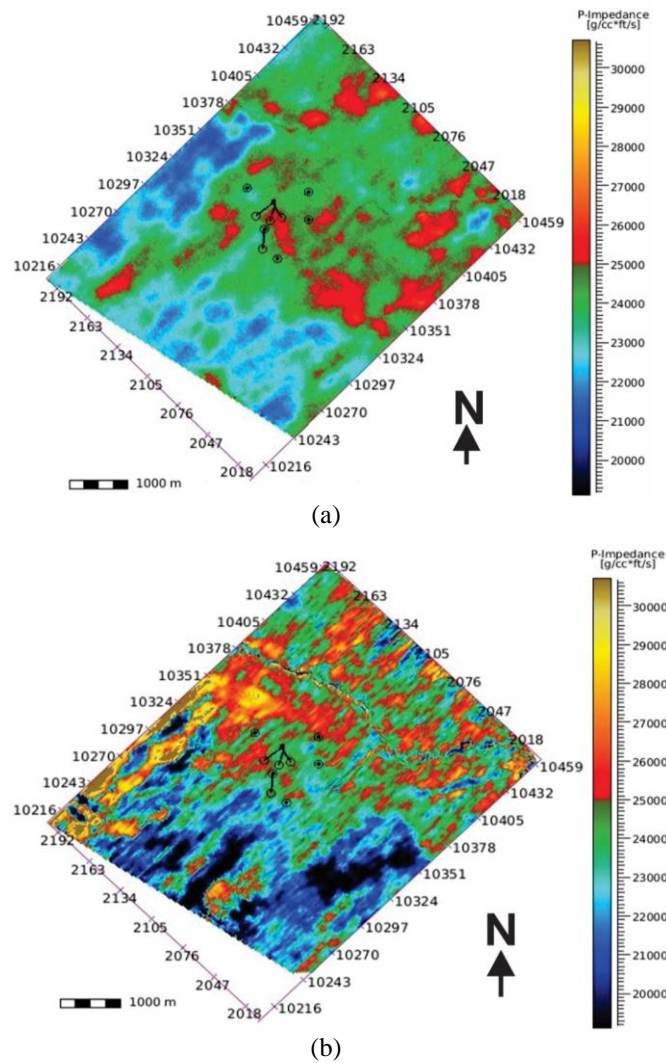
Figure 7 The P-impedance map along layer M, which was produced by: (a) geostatistical seismic inversion; and (b) deterministic seismic inversion

The advantage of the discrete properties model compared to inverted P-impedance was that the discrete properties model was able to clearly delineate between the target zone and non-target zone. This means that not the entire delineated target zone in the inverted P-impedance was classified as a target zone in the discrete properties model. This model was the average of 50 inverse realizations. The probability of the discrete properties model was higher in the area that was close to a well.

The detailed analysis of the inverted P-impedance is illustrated in the P-impedance map. Figure 7 shows the P-impedance map of layer M, which was produced by the geostatistical seismic inversion and deterministic seismic inversion. The significant difference was clearly identified in the distribution of the target reservoir, where the geostatistical seismic inversion illustrated continuous target zone (Figure 7a) rather than the deterministic seismic inversion (Figure 7b). The distribution of the thin reservoir is indicated by the red area inside the circle. The thin reservoir represents the sand lenses in the high structure. The red area indicates hydrocarbon potential.

4. CONCLUSION

Geostatistical seismic inversion has been successfully applied to the thin reservoir of the Air Benakat formation in the Jambi sub-basin by producing high vertical resolution and accurately mapping sub-seismic features of the thin reservoir rather than by using the deterministic seismic inversion. The reservoir target was identified as glauconitic sandstone with a relatively high P-impedance, which was based on the cross-plot analysis. The geostatistical seismic inversion model was not limited to the tuning thickness of seismic data, as it was based on simulations by considering the PDF and variogram model. In addition, the geostatistical seismic inversion was constrained by the probability model and the discrete properties model, which was useful in delineating between the target zone and non-target zone. The detailed analysis of the inverted P-impedance showed that the geostatistical seismic inversion illustrates continous target zone rather than the deterministic seismic inversion. The thin layer distribution was indicated by the high P-impedance with the certainty of 60%, which was based on the simulation model run 50 times.

5. ACKNOWLEDGEMENT

6. REFERENCES

Avseth, P., Mukerji, T., Mavko, G., 2005. *Quantitative Seismic Interpretation: Applying Rock Physics Tools to Reduce Interpretation Risk*. Cambridge: Cambridge University Press

Bacon, M., Simm, R., Redshaw, T., 2003. *3-D Seismic Interpretation*. Cambridge: Cambridge University Press

Bishop, M.G., 2001. *South Sumatera Basin Province, Indonesia: The Lahat/Talang Akar-Cenozoic Total Petroleum System*. Denver: United States Geological Survey

Bosch, M., Mukerji, T., Ezequiel, F.G., 2010. Seismic Inversion for Reservoir Properties Combining Statistical Rock Physics and Geostatistics: A Review. *Geophysics*, Volume 75(5), pp. 75A165–75A176

Francis, A.M., 2005. Limitation of Deterministic and Advantages of Stochastic Seismic Inversion. *Recorder*, Volume 30(2), pp. 5–11

Francis, A.M., 2006. Understanding Stochastic Inversion: Part 1. *First Break*, Volume 24(11), pp. 69–77

Ginger, D., Fielding, K., 2005. The Petroleum Systems and Future Potential of the South Sumatra Basin. *In*: The 30th Annual Indonesian Petroleum Association Conference Proceedings

Haas, A., Dubrule, O., 1994. Geostatistical Inversion: A Sequential Method of Stochastic Reservoir Model Constrained by Seismic Data. *First Break*, Volume 12(11), pp. 561–569

Haris, A., Murdianto, B., Susattyo, R., Riyanto, A., 2018. Transforming Seismic Data into Lateral Sonic Properties using Artificial Neural Network: A Case Study of Real Data Set. *International Journal of Technology*. Volume 9(3), pp. 472–478

Haris, A., Novriyani, M., Suparno, S., Hidayat, R., Riyanto, A., 2017. Integrated Seismic Stochastic Inversion and Multi-attributes to Delineate Reservoir Distribution: Case Study MZ Fields, Central Sumatra Basin. *AIP Conference Proceedings.* Volume 1862(1), pp. 030180-1–030180-4

Havelia, K., Aly, O., Mukherjee, A., Zeng, R., Nyein, G., Figuera, L.G., Aamir, M., Al Hosani, K.M., Alkatheeri, F., Al Raeesi, M., Al Hamedi, A., 2017. Characterization of the Lower Cretaceous Thamama Group Reservoirs through Stochastic Inversion and Rock Physics Modeling. *In*: Fourth EAGE Workshop on Rock Physics 2017 Nov 11

Hermana, M., Ghosh, D.P., Sum, C.W., 2017. Discriminating Lithology and Pore Fill in Hydrocarbon Prediction from Seismic Elastic Inversion using Absorption Attributes. *The Leading Edge*, Volume 36(11), pp. 902–909

Lang, X., Grana, D., 2017. Geostatistical Inversion of Prestack Seismic Data for the Joint Estimation of Facies and Impedances using Stochastic Sampling from Gaussian Mixture Posterior Distributions. *Geophysics*, Volume 82(4), pp. M55–M65

McCrank, J., Lawton, D., Mangat, C., 2009. *Geostatistical Inversion of Seismic Data from Thinly Bedded Ardley Coals*. CSPG CSEG CWLS Convention. Calgary, Alberta, Canada

Mukerji, T., Jørstad, A., Avseth, P., Mavko, G., Granli, J.R., 2001. Mapping Lithofacies and Pore-fluid Probabilities in a North Sea Reservoir: Seismic Inversions and Statistical Rock Physics. *Geophysics*, Volume 66(4), pp. 988–1001

Nunes, R., Soares, A., Azevedo, L., Pereira, P., 2017. Geostatistical Seismic Inversion with Direct Sequential Simulation and Co-simulation with Multi-local Distribution Functions. *Mathematical Geosciences*, Volume 49(5), pp. 583–601

Robinson, G., 2001. Stochastic Seismic Inversion Applied to Reservoir Characterization. *Canadian Society of Exploration Geophysicists Recorder*. Volume 26(1), pp. 36–40

Sams, M., Saussus, D., 2010. Comparison of Lithology and Net Pay Uncertainty between Deterministic and Geostatistical Inversion Workflows. *First break*, Volume 28(2), pp. 35–44

Sancevero, S.S., Remacre, A.Z., Mundim, E.C., de Souza Portugal, R., 2008. Application of Stochastic Inversion to Reservoir Characterization Process. *Earth Science Frontiers*, Volume 15(1), pp. 187–195

Shrestha, R.K., Boeckmann, M., 2002. Stochastic Seismic Inversion for Reservoir Modeling. *In*: 2002 SEG Annual Meeting. Society of Exploration Geophysicists

Sulistiono, D., Vaughan, R., Ali, M. Rasoulzadeh, S., 2015. Integrating Seismic and Well Data into Highly Detailed Reservoir Model through AVA Geostatistical Inversion. *In*: Abu Dhabi International Petroleum Exhibition and Conference. Society of Petroleum Engineers

Torres-Verdin, C., Victoria, M., Merletti, G., Pendrel, J., 1999. Trace-based and Geostatistical Inversion of 3-D Seismic Data for Thin-sand Delineation: An Application in San Jorge Basin, Argentina. *The Leading Edge*, Volume 18(9), pp. 1070–1077